

REVIEW PAPER

## Experimental Techniques for the Measurement of Mechanical Properties of Materials Used in Microelectromechanical Systems

Samir V. Kamat

*Defence Metallurgical Research Laboratory, Kanchanbagh, Hyderabad-500 058*  
*E-mail: kamat@dmrl.drdo.in*

### ABSTRACT

The knowledge of mechanical properties of materials used in microelectromechanical systems (MEMS) devices is critical not only in designing structures such as cantilevers and beams but also for ensuring their reliability during operation of these devices. It has been established that the mechanical properties are scale-and-process-dependent, and hence it is essential to measure the mechanical properties of these materials at the same length scale and using the same process as that used in their usage in MEMS devices. The various experimental techniques in vogue to measure the mechanical properties of these materials are briefly reviewed. The facilities established at the Defence Metallurgical Research Laboratory, Hyderabad, and their capabilities are also highlighted.

**Keywords:** Mechanical properties, MEMS, microelectromechanical systems, experimental techniques

### 1. INTRODUCTION

The past two decades have seen the emergence and rapid growth of microelectromechanical systems (MEMS) as an important area of technology with possible applications in defence as well as in the civilian sector. The basic premise behind the concept of MEMS is that the efficiencies of high volume production and low unit cost achieved by the microelectronics industry over the past 50 years can be translated to devices in which the mechanical and electrical/electronic functions are integrated. In addition to the potential economic benefits, unique capabilities can be achieved by such integration to realize devices at very small scales such as sensors<sup>1-6</sup>, actuators<sup>1,7-10</sup>, power producing devices<sup>11-13</sup>, chemical reactors<sup>14-16</sup> and biomedical devices<sup>17-20</sup>. The potential military applications for MEMS<sup>21</sup> include those in personnel systems, inertial guidance systems in precision-guided munitions, health monitoring of aircraft engine and structures, microUAVs, picosatellites, light weight radios, etc.

Most new technologies tend to originate with new materials and manufacturing processes that are used to create new products. In the initial stages, the emphasis is usually on novel devices and systems and ways of making them. Studies on fundamental issues such as mechanical properties and their correlation to the microstructure usually happen at a much later stage. The same is true for MEMS. It is only in the last few years that sustained efforts are being made to characterize and understand the mechanical properties of MEMS structures and materials. The issue here is that microfabricated materials have properties that are highly dependent on the fabrication route used

to create them and the scale of the structures that they constitute. The mechanical properties at the microscale can vary considerably from those measured on bulk samples of materials at the macroscale. Even properties such as density and elastic modulus, which are not inherently scale-dependent, can be altered from bulk values in deposited layers by the creation of non-equilibrium microstructures, dissolved gases from vapour deposition and the influence of the substrate. To fully realise the potential for accurate and rapid simulation tools for the design of MEMS, models are required which link the property achieved to the fabrication route and material used. The first step towards this is to develop standard test methods with which to characterise the mechanical properties of microfabricated materials produced by the same processes and at the same scales as the intended applications. This will enable the creation of validated material property and process databases and correlations between processing routes and properties, to permit simulation-based design. Some of the key mechanical properties which need characterisation are elastic properties, room and elevated temperature strengths, fracture toughness and fatigue behaviour.

The paper aims to review the test techniques used to characterise the materials used in MEMS as well as to highlight the facilities that have been set-up at the DMRL to characterise the mechanical properties. There have been other reviews published<sup>22-28</sup>.

### 2. TEST METHODS

In conventional studies of mechanical behaviour of materials, it is a common practice to create test samples

of the materials in question, subject these to forces and displacements, and measure the corresponding response. Usually, simple stress states, such as tension, compression, torsion and bending, are used to permit the calculations of stress and strain from the measured forces and displacements. Such an approach cannot be used to study the mechanical behaviour of materials used in MEMS because of the difficulties associated with specimen fabrication and handling as well as the extremely small loads and displacements involved in such cases. It should also be noted that mechanical behaviour of materials cannot simply be deduced from the mechanical behaviour of bulk samples, since mechanical behaviour is controlled by length scales<sup>29</sup>, which are inherent to the respective physical mechanisms. In bulk materials, the sample dimensions usually do not interfere with fundamental lengths, but in thin film samples, as used in MEMS, the geometrical as well as the microstructural dimensions are typically of the same order of magnitude, and hence, it is expected that the mechanical properties of the material will be affected by sample dimensions.

In recent years, the development of depth-sensing nanoindentation instruments as well as advances in fabrication techniques has resulted in a quantum jump in the methods for characterisation of the mechanical behaviour of materials used in MEMS. Current methods include depth-sensing nanoindentation, microbeam bending, microtensile testing, bulge testing, x-ray diffraction, and substrate curvature measurement. Elastic, plastic, creep, fatigue, fracture toughness, interfacial toughness as well tribological properties can be determined utilising these techniques, but the various methods are not equally well applicable to determine any characteristic quantity. Some of the critical issues for each technique are highlighted.

## 2.1 Nanoindentation

Depth-sensing nanoindentation is by far the most commonly used technique for characterisation of mechanical behaviour of materials used in MEMS even though the stress state beneath the indentation is complex. This is because of its relative simplicity and no additional requirement of specimen fabrication and preparation. Nanoindentation has been used to determine elastic properties, hardness, plastic properties, fracture toughness, interfacial toughness, fatigue, creep, friction coefficient as well as residual stresses in films patterned to make MEMS structures such as cantilevers and beams, prior to their release from the substrate. An exhaustive overview of the nanoindentation technique is provided by Bhushan and Li<sup>30</sup>, and hence, this is only briefly covered in this review. The main information that one gets from a nanoindentation test is the load versus depth of penetration during the indentation process. A typical load versus depth of penetration of the indenter or  $P$ - $h$  plot for a sharp indenter is shown in Fig. 1.

The elastic modulus and hardness can be calculated from this plot using the well known procedure suggested by Oliver and Pharr<sup>31</sup>. The calculation of fracture toughness, interface toughness, fatigue ( $S$ - $N$  curve), creep and friction

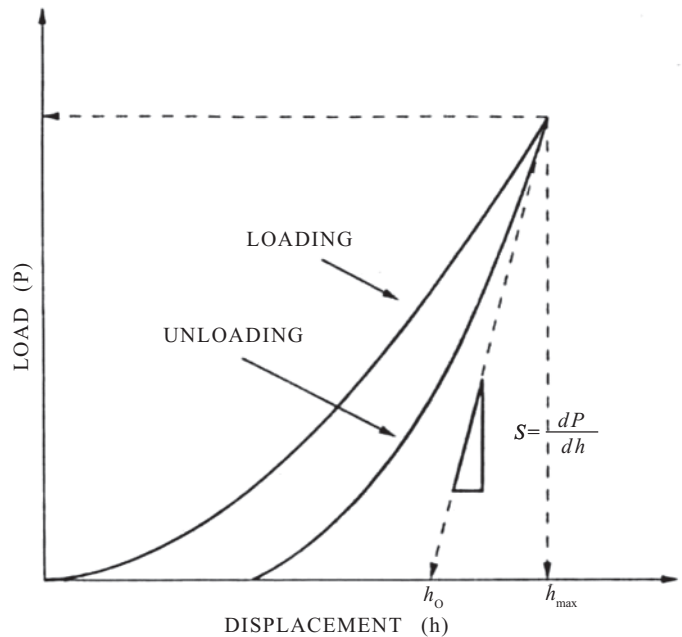


**Figure 1. Typical load versus depth of penetration plot from a nanoindentation test.**

coefficient is also discussed in detail in the review by Bhushan and Li<sup>30</sup>.

Most commercial nanoindenters also have an atomic force microscope (AFM) as an attachment which can be used to image the indentation as well as study the deformation around the indentation. Several types of indenters are used. The most common is the three sided pyramidal indenter commonly known as the Berkovich indenter. Other type of indenters, such as spherical, conical, cube corner or flat ended cylindrical punch indenters, are also used in cases where specific properties need to be measured.

## 2.2 Uniaxial Tensile Testing

The equivalent of a tensile test performed on a bulk sample is desirable for thin films used in MEMS devices because the stress and strains in a tensile test are uniform and they can be measured directly and independently. Hence, no mathematical assumptions are needed to calculate the elastic and plastic properties from the experimental data. There are three issues in tensile testing – specimen preparation, force application, and strain measurement<sup>32</sup>. Each issue takes on a new level of difficulty if the specimen is thin and small. One cannot machine a tensile specimen, pick it up, and place it in a set of grips if the material is very thin (say a few microns thick) and the specimen is small.

Once the tensile specimen size is smaller than a few millimeters, one cannot use traditional gripping methods such as threaded ends, pin and hole connections, or compression grips. A solution is to make the specimen in the shape of a ‘dog bone’, i.e., with wedge-shaped ends with the test section in the middle<sup>33,34</sup>. Figure 2 is a photograph of a LIGA nickel specimen with this shape. The ends are large enough that matching inserts can be machined into the

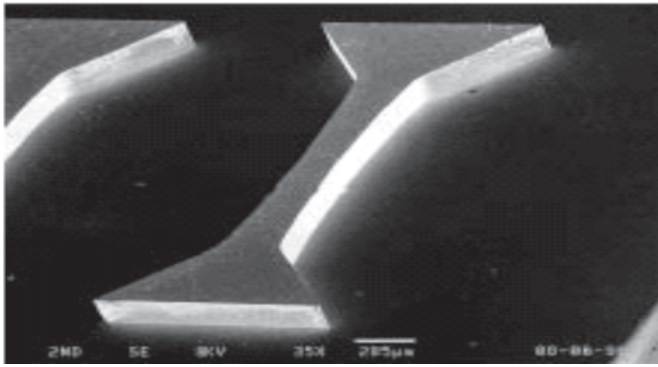


Figure 2. A dog bone LIGA nickel microtensile specimen<sup>33</sup>.

grips. The specimen is simply placed in the inserts, and friction along the V-shaped sides holds it in place. This works well with ductile materials where local yielding can accommodate any misalignment or stress concentration.

Another approach, particularly useful with very thin materials, is to remove the substrate to reveal a free-standing tensile region. There are earlier demonstrations, but Read and Dally<sup>35</sup> introduced a version that is used for MEMS materials; Fig. 3 is an example<sup>36</sup>. The tensile specimen in the centre is silicon nitride that is 0.5  $\mu\text{m}$  thick and 600  $\mu\text{m}$  wide. It was deposited on the other side of the 1  $\text{cm}^2$  silicon die shown in the figure. The front surface was protected, and rectangular window was etched into the visible back side.

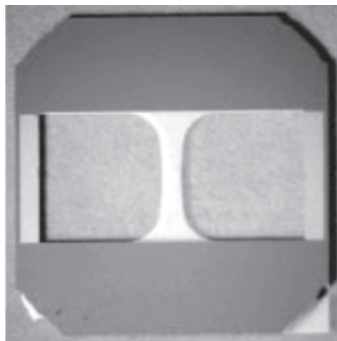


Figure 3. Silicon nitride specimen-0.5  $\mu\text{m}$  thick by 600  $\mu\text{m}$  wide in a silicon frame<sup>36</sup>.

This creates a frame across which the specimen is supported. It is easy to handle the frame and glue the wide top and bottom pieces into the grips of a test machine. The narrow side support strips are then cut with a diamond saw to leave a completely free tensile specimen. This kind of specimen is robust and has several advantages, but is expensive in that only one specimen is produced per one-cm square die. Further the release process can be time consuming.

A different approach was introduced by Tsuchiya<sup>37</sup>, *et al.* and Fig. 4 is a photograph of a specimen based on their work<sup>38</sup>.

The right end of the specimen remains fastened to the substrate, which appears black in the photograph. The rest of the structure is freed from the substrate by etching



Figure 4. Polysilicon tensile specimen-3.5  $\mu\text{m}$  thick, 50  $\mu\text{m}$  wide, and 2 mm long<sup>36</sup>.

away the underlying oxide film. Each holes are provided in the wide paddle end at the left and in the curved regions at the ends of the straight test section. The four anchor straps on the grip end prevent damage while the die is being handled; these are broken with a microprobe before testing. A single 1  $\text{cm}^2$  die can contain 10-20 of these specimens. The left end of the specimen in Fig. 4 can be gripped with an electrostatic probe as Tsuchiya<sup>37</sup>, *et al.* showed, and Fig. 5 is a photograph of the arrangement. The single crystal silicon probe on the left had a wire attached to its top and an insulating layer of nitride on its bottom. A voltage (50-200 V) is applied across this insulating layer via the wire and the probe on the right. This attracts the grip end of the specimen to the probe with enough force and enough friction to pull the specimen. Once setup, this is an especially easy-to-use gripping mechanism. However, it is not strong enough to break larger polysilicon specimens. A process for gluing silicon carbide fibres 140  $\mu\text{m}$  in diameter to the grip end were developed<sup>38</sup>. Although more time-consuming, that is also a straightforward method.

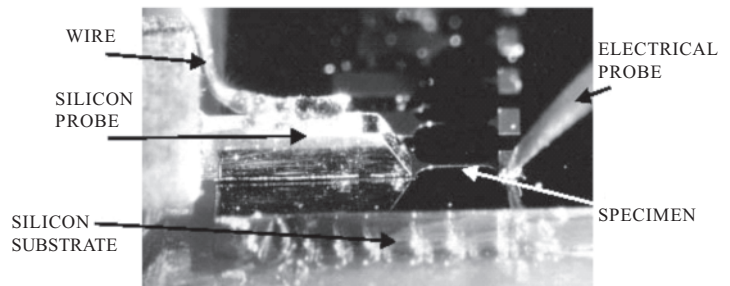


Figure 5. Electrostatic probe gripping a narrow polysilicon specimen<sup>37</sup>.

Even easier still is a ring grip on the end of the specimen; one simply inserts a pin into the hole<sup>39</sup>. Figure 6 shows specimens of this design. The material here is a composite of aluminum and silicon dioxide as used in an ordinary CMOS process. Manufacturing MEMS by this process has potential advantages because of the easy integration of mechanical components with electronics. These are new specimens and test method development has been initiated.

The force required to break a 2  $\mu\text{m}$   $\times$  2  $\mu\text{m}$  specimen with fracture strength of 1 GPa is 4 mN or  $\sim$  0.4 g. That is not so hard to measure, as 5 g load cells are commercially available. The elongation of such a specimen, if it is 100  $\mu\text{m}$  long and Young's modulus is 150 GPa, is only  $\sim$  0.7  $\mu\text{m}$ . That is not so hard either; commercial actuators and displacement

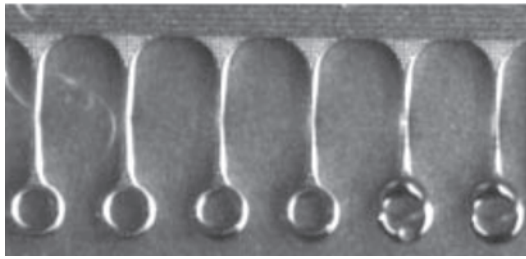


Figure 6. CMOS specimens with rings on the grip ends<sup>37</sup>.

sensors with resolutions in the 0.01 mm range are available. The challenge is putting these together as a useful test system. A more-or-less traditional approach can be used for the larger specimens as shown in Fig. 2. The main issue is reducing the friction in the alignment mechanism of the movable grip. This is accomplished with a linear air bearing and has proved to be quite successful. Figure 7 shows the setup for the larger thin-film specimens. This is basically the same arrangement as used for the LIGA specimens. The load cell has a 4.45 N capacity and the actuator has a 180  $\mu\text{m}$  range. If the specimen is smaller, as in Fig. 15, the probe or fibre attached to the grip end can be aligned to pull the specimen along its tensile axis. This is more difficult with the electrostatic probe because there are always some inaccuracies in the positioning of the die with the specimens on it. That die is mounted on a five-axis piezoelectric stage, which permits one to align the specimen while observing it from the front with a low-power stereomicroscope, and from the side with a telemicroscope. The probe and the load cell are mounted on a single-axis piezoelectric stage operated under computer control to pull the specimen<sup>40</sup>. The glued fibre is several millimeter long and attached directly to a 1 N load cell mounted on a single-axis piezoelectric stage. That stage is attached to a three-axis manual stage, which is used to position the fibre for gluing and to align for axial loading<sup>38</sup>.

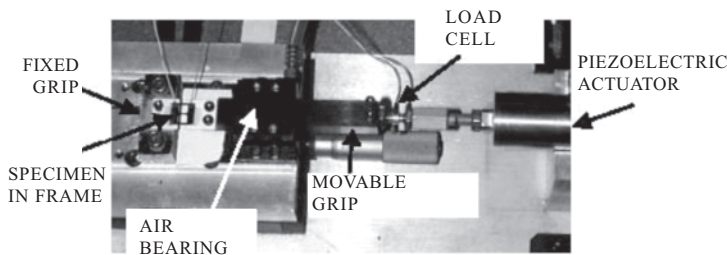


Figure 7. Test system for larger specimens<sup>40</sup>.

A traditional stress-strain test calls for direct measurement of strain on the specimen. This is very easy to do if the specimen is large; foil strain gages or clip gages are used. If the specimen is very long, such as a wire, the relative displacements of the grip ends can be used to compute the strain. Neither of these measurements – direct or displacement – are easy to make on thin and small specimens, although both have been accomplished. One approach is to make the specimen relatively long in the gage section and test it in

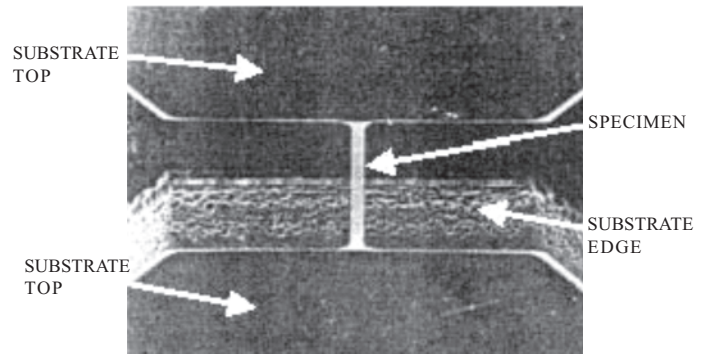


Figure 8. Thin aluminum specimen across substrate grips<sup>41</sup>.

a loading system that is very stiff. Strain can be calculated from the differential displacement. One example of that approach is shown in Fig. 8<sup>41</sup>. The aluminum specimen is 2  $\mu\text{m}$  thick, 50  $\mu\text{m}$  wide, and 500  $\mu\text{m}$  long.

It is almost always desirable, but not always possible, to measure strain directly in the gage section as ASTM requires. One way to do this is to apply reflective markers (in effect, gage points) to the specimen and use laser interferometry from them to measure the strain. This approach, known as the interferometric strain displacement gage (ISDG), has been used extensively to test thin ceramic films and thicker electroplated nickels<sup>42,43</sup>. The reflective markers are vapour-deposited gold lines, shown in Fig. 9(a) or microhardness indentations, shown in Fig. 9(b).

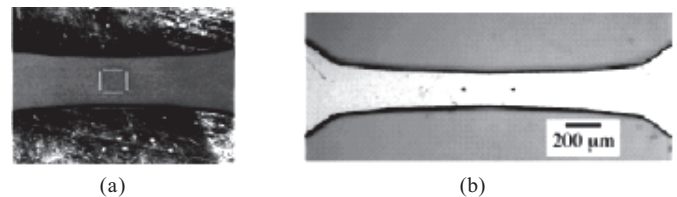


Figure 9. (a) Gold reflective markers on a polysilicon specimen, and (b) microhardness indentations in a nickel specimen<sup>42</sup>.

Protruding flags can also be molded on the gage section of nickel specimens and the relative displacement measured with a laser scanning system<sup>44</sup>. The optimal situation would be simply to use digital image correlation with an optical microscope. That is possible, but still very slow<sup>45</sup>.

Espinosa<sup>46</sup>, *et al.* have developed a novel  $\mu$ -scale membrane deflection experiment particularly suited for the investigation of submicron thin films and MEMS materials. The experiment consists of loading a fixed-fixed membrane (Fig. 10) with a line load that is applied to the middle of the span with a nanoindenter column which results in a tensile load on both the specimens. A Mirau microscope-interferometer is positioned below the membrane to observe its response to loading (Fig. 11).

This is accomplished through a specially micromachined wafer containing a window to expose the bottom surface of the membrane. The sample stage incorporates the interferometer to allow continuous monitoring of the membrane deflection during both loading and unloading. As the nanoindenter

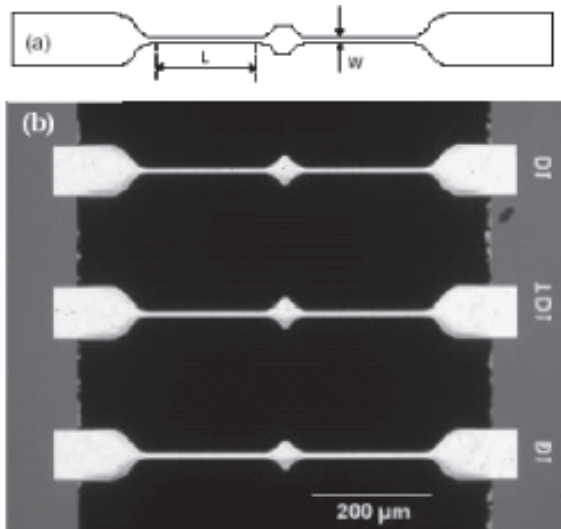


Figure 10. (a) Schematic view of the membrane specimens where  $L = 200 \mu\text{m}$  and  $W = 20 \mu\text{m}$ , and (b) optical image of microfabricated membrane specimens<sup>46</sup>.

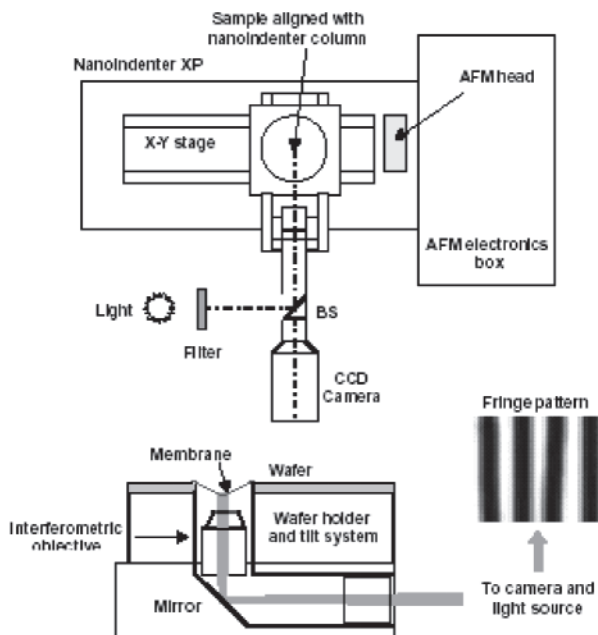


Figure 11. Schematic of combined AFM/nanoindenter testing rig with integrated Mirau microscope-interferometer deflection test<sup>46</sup>.

engages and deflects the sample downward, fringes are formed due to the motion of the bottom surface of the membrane and are acquired through a CCD camera. Digital monochromatic images are obtained and stored at periodic intervals of time to map the strain field. Through this method, loads and strains are measured directly and independently without the need for mathematical assumptions to obtain the necessary parameters for describing material response. They have demonstrated this testing scheme by measuring the stress-strain curve for a gold membrane (Fig. 12)<sup>46</sup>. The critical concern in this membrane deflection

experiment (MDE) is accounting for the thermal drift and spring constant of the nanoindenter column. Since the column dimension is orders of magnitude larger than the membrane deflection, subtle changes in temperature can significantly affect displacement measurement. To account for these two factors, they made indents on either post supporting the membrane. Corrections for thermal drift and spring constant are calculated from the approach segment data before contact with the posts. Other important information is also gained from these indents such as: device tilt, height of the membrane at contact, and middle position in the plane of the film. The load-displacement data can then be adjusted accordingly.

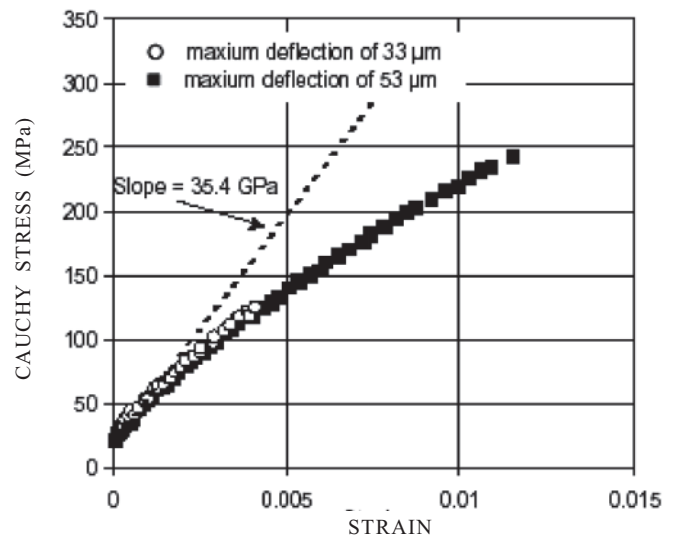


Figure 12. Cauchy stress versus strain for an *Au* membrane  $0.5 \times 20 \mu\text{m}$  cross-section. Modulus was found to be  $35.4 \text{ GPa}$ <sup>46</sup>.

### 2.3 Microbeam Bending

Microbeam deflection experiments using a nanoindenter are well established for determining yield stress and elastic stiffness of materials used in MEMS at the same length scale<sup>47-50</sup>. In this technique, very small cantilever beam specimens (Fig. 13) are used which are produced by surface or bulk micromachining techniques.

A nanoindenter with a wedge-type indentation is used to load the beam at the free end (Fig. 14) and it records both the load as well as displacement.



Figure 13. Micrograph of a beam array made by micro-machining<sup>47</sup>.

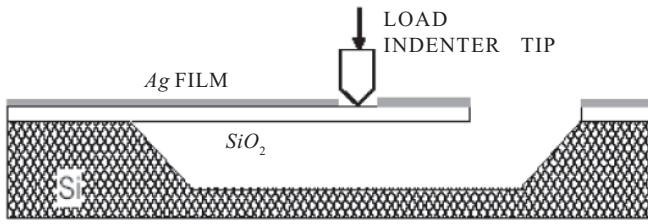


Figure 14. Schematic of the microbeam loading using a nanoindenter<sup>47</sup>.

A representative load versus displacement plot<sup>47</sup> is shown in Fig. 15. The elastic modulus and the yield strength of the material can be determined from the load deflection curve using beam theory or FEM<sup>47-50</sup>. This technique can also be extended for measuring the fatigue response of the films by superimposing an oscillating signal along with the monotonic force signal and using the continuous stiffness monitoring option of the nanoindenter system<sup>51</sup>.

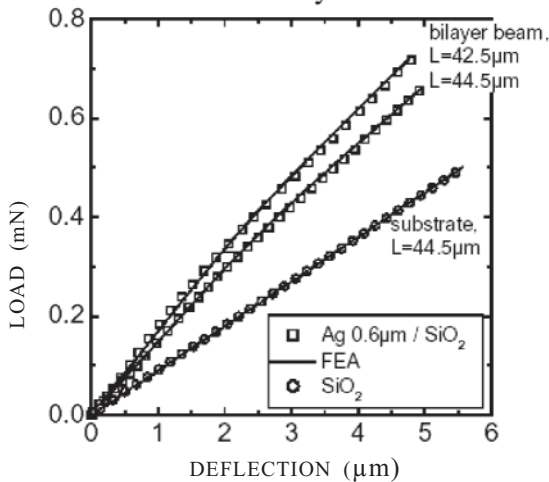


Figure 15. Load deflection plot for a  $Ag/SiO_2$  bilayer beam<sup>47</sup>.

### 2.4 Bulge Test

The bulge test is another commonly used technique for measuring the mechanical properties of materials used in MEMS. In the bulge test<sup>52-54</sup>, a freestanding thin film is deflected by applying a uniform pressure to the film. The schematic of the bulge test specimen is shown in Fig. 16. The thin film membrane is initially flat. As the membrane deflects, the film experiences an in-plane strain. By measuring the pressure ( $P$ ) and the deflection ( $h$ ) at the centre of the membrane, the in-plane stress and strain can be determined. Elastic, plastic, and time dependent properties of the film can thus be obtained. One of the advantages of the technique is that strain can be changed quickly and isothermally, and that large strains can be imposed. For a long rectangular membrane, the deformation can be taken as plane strain in the center part of the membrane. The in-plane stress and strain can then be calculated from the pressure-deflection data using the following simple formulae<sup>53</sup>

$$\sigma = \frac{Pa^2}{2ht} \quad \text{and} \quad \varepsilon = \varepsilon_0 + \frac{2h^2}{3a^2} \quad (1)$$

where,  $t$  is the film thickness,  $2a$  is the width of the membrane, as shown in Fig. 16, and  $\varepsilon_0$  is residual strain. Equation (1) is accurate for strains  $< 1$  per cent. A typical plot from a bulge test of  $Cu$  films on  $Si$  substrate as shown in Fig. 17.

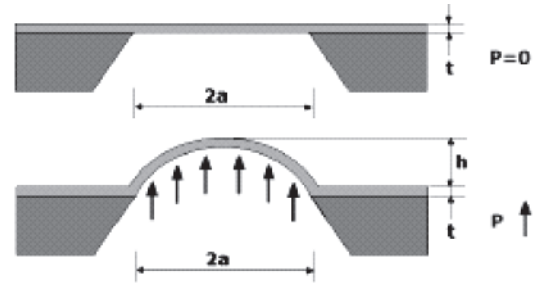


Figure 16. Schematic of the bulge test and the apparatus<sup>52</sup>.

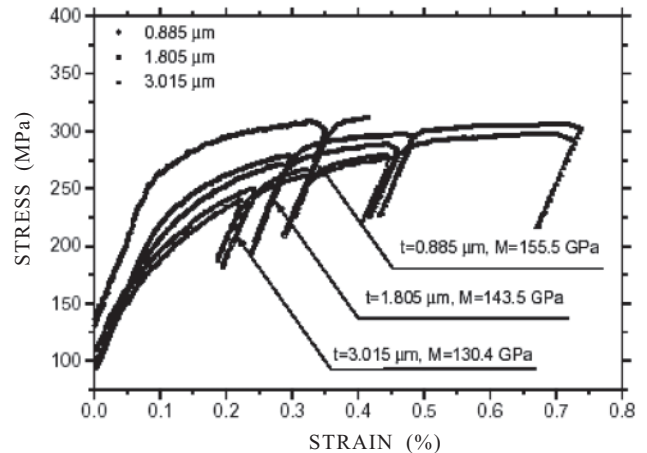


Figure 17. Stress-strain curves for copper films of different film thickness from a bulge test<sup>52</sup>.

### 2.5 Film-substrate Combinations Subjected to Thermal Stress

Another technique which has been used for measuring the mechanical properties of materials used in MEMS involves using thermal expansion and substrate curvature methods for certain film-substrate combinations<sup>55,56</sup>. When the temperature of the bilayer beam is changed, the difference in thermal expansion between the film and the substrate sets up internal biaxial stresses in the composite which vary with the temperature such that<sup>55</sup>:

$$\frac{d\sigma}{dT} = \frac{E}{(1-\nu)} \Delta\alpha \quad (2)$$

where,  $T$  is the temperature and  $\Delta\alpha$  is the difference between the thermal expansion coefficients of the film and the substrate. The radius of curvature,  $R$ , is related to the stress in accordance with

$$\sigma = \left( \frac{E}{1-\nu} \right)_s \frac{h_s^2}{6Rh_f} \quad (3)$$

Here the subscript  $s$  and  $f$  refer to the substrate and film, respectively. In general, the film in the as-received condition is subjected to an annealing treatment in order to stabilise the grain structure. Because of the relatively high expansion coefficient of metallic materials, the annealed film is in a state of tension on cooling to room temperature. Subsequent heating lowers the tensile stresses and eventually creates a state of compression in the film (Fig.18).

The slope of the biaxial stress-temperature curve is given by Eqn (2). As shown in Fig. 18, the inception of plastic deformation in biaxial compression is clearly noticeable as the curve deviates from linearity. Using this technique Doerner<sup>55</sup>, *et al.* were able to demonstrate that an increasing thickness of aluminium films deposited on silicon was associated with lower strength.

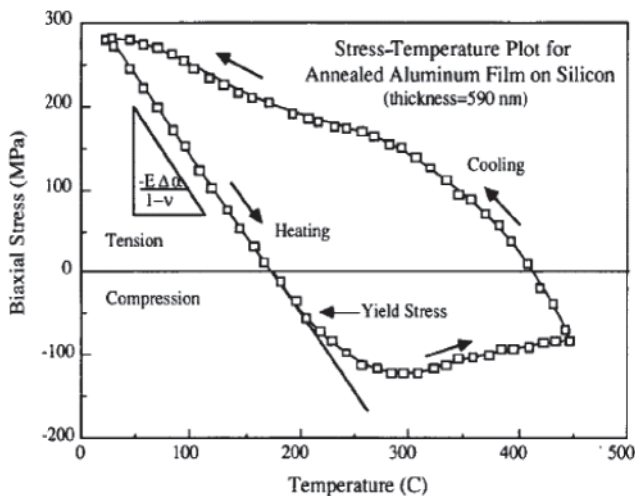


Figure 18. Stress-temperature plot for annealed Al film on Si substrate<sup>52</sup>.

## 2.6 Fatigue

The study of fatigue behaviour of materials used in MEMS is critical to understand the reliability of MEMS. Muhlstein<sup>57</sup>, *et al.* have developed a specimen geometry and test structure for characterisation of fatigue crack initiation in thin films and have explored fatigue crack initiation in a variety of materials systems. The structure design is based on the philosophy that underlies fatigue testing standards such as ASTM E 466. The micron-scale fatigue characterisation structure shown in Fig. 19 is approximately  $300 \mu\text{m}^2$ . This structure is analogous to a specimen, electromechanical load frame, and capacitive displacement transducer found in a conventional mechanical testing system. The specimen is a notched cantilever beam that is in turn attached to a large, perforated plate that serves as a resonant mass. The mass and beam are electrostatically forced to resonate and the resulting motion is measured capacitively. On opposite sides of the resonant mass are interdigitated fingers, commonly referred to as comb drives.

One side of these drives is for electrostatic actuation; the other side provides capacitive sensing of motion. The specimen is attached to an electrical ground, and a sinusoidal voltage at the appropriate frequency is applied to one comb drive, thereby inducing a resonant response in the plane of the figure. The opposing comb drive is attached to a constant potential difference, and the relative motion of the grounded and biased fingers induces a current proportional to the amplitude of motion. The small induced current is converted to a direct current (dc) voltage using an analog circuit. A variety of circuits for capacitive sensing can be found in the literature<sup>58</sup>.

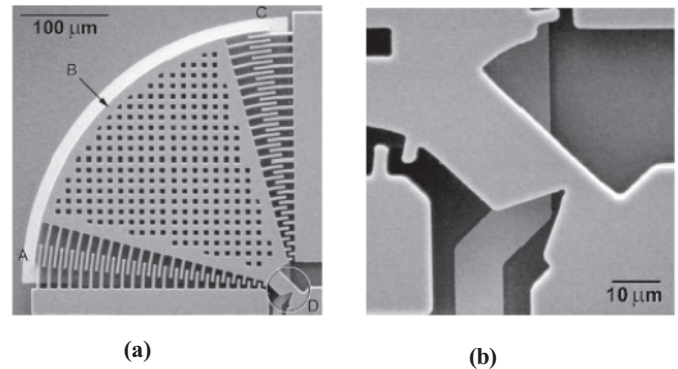


Figure 19. SEM of the stress-life fatigue characterisation structure: (a) electrostatic comb drive actuator (A), resonant mass (B), capacitive displacement transducer comb (C), and notched cantilever beam specimen (D), and (b) A detail of the notched beam<sup>57</sup>.

The output of the circuit used in this study was calibrated using the computer microvision system developed by Freeman<sup>59</sup> and stresses at the notch were calculated using the commercial finite element analysis package ANSYS. The radius of the stress concentration and the remaining beam ligament were selected to ensure that the specimen could be broken immediately at resonance. The longer-term fatigue response can then be measured by exciting the specimen at some fraction of the short time breaking amplitude. All samples were tested until failure occurred by fracture of the beam at the notch. The resonant frequency is used to monitor the accumulation of fatigue damage in the specimen until failure occurs at the notch.

The device was driven at resonance using the following control scheme:

- The first mode resonant response of the specimen is determined by sweeping a range of frequencies around the expected response and monitoring the amplitude of response.
- The peak amplitude is selected by fitting a second-order polynomial to the peak and extracting the maximum.
- The specimen is then excited at the peak frequency at a defined excitation voltage for a period of time.
- The frequency response is then again evaluated by sweeping around the excitation frequency. Over time this permits measuring any change in resonant frequency

and consequently any change in the mechanical response of the specimen.

This scheme is simple yet effective in detecting the compliance changes associated with crack growth and damage accumulation. The same set-up can also be used to measure the conventional S-N curves by using smooth specimens instead of notched specimens. In recent times, other fatigue test specimens and test systems have also been developed to study the fatigue behaviour of thin films<sup>60-62</sup>.

### 3. FACILITIES ESTABLISHED AT DMRL

The brief overview above has highlighted the various test techniques for determining the mechanical properties of materials used in MEMS devices. In this section the facilities and capabilities for characterising the mechanical properties of MEMS materials established at Defence Metallurgical Research Laboratory, Hyderabad is presented:

#### (a) Nanoindenter

Nanoindenter both as an indenting tool for determining mechanical properties such as elastic properties, hardness, plastic properties, fracture toughness, creep, fatigue and friction coefficient as well as a loading tool for conducting microbeam bending and membrane deflection tests to determine yield strength and fatigue properties has been established.



Figure 20. Nanoindenter.

The salient features of the nanoindenter are:

- Load range: 1 mN - 100 mN (low load) and 100 mN-5000 mN (high load)
- Maximum indentation depth: 20  $\mu\text{m}$
- Minimum displacement of X-Y table: 100 nm
- Temperature capability from room temperature to 200 °C
- Static and cyclic loadings
- Berkovich, spherical and conical tips of varying tip radius
- Mirau interferometer capable of measuring strain or deflection directly on the specimen.

#### (b) Microtensile tester

Microtensile tester for testing relatively larger MEMS specimens (especially LIGA) (Fig. 21).

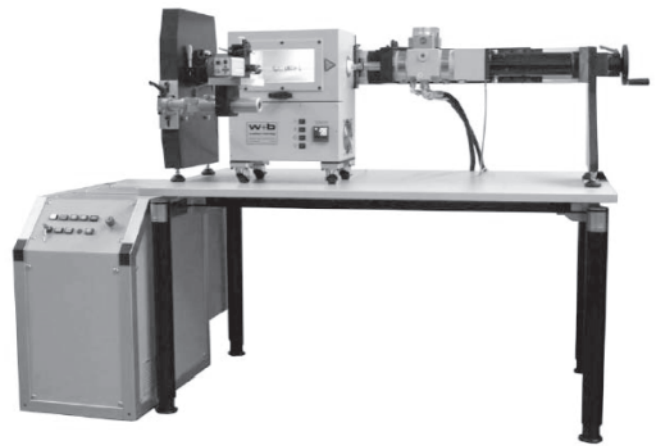


Figure 21. Microtensile test system.

The salient features of the microtensile test system are:

- Static and dynamic testing up to 500 N load and 30Hz frequency,
  - Environmental chamber for room temperature to 250°C
  - Laser speckle extensometer for direct measurement of strain.
- (c) Laser Scanning Equipment
- Laser scanning equipment for measuring elastic modulus and elastic-plastic properties of films on a substrate (Fig. 22).



Figure 22. Laser scanning thin film stress measurement system.

The salient features of laser scanning thin film stress measurement system are:

- Dual-wavelength laser system (of wavelengths 670 nm and 780 nm)
- Fast data acquisition with the speed of 5 sec for 150 mm wafer
- High resolution of 0.00003  $\text{m}^{-1}$
- Two-dimensional mapping of residual stress
- Temperature range from -50 °C to 450 °C.

### 4. SUMMARY

It is important and necessary to measure mechanical properties of materials used in MEMS at the same length scales as their usage in the device for design as well as reliability of MEMS structures. The experimental techniques for the measurement of mechanical properties of materials

used in MEMS were briefly reviewed. The facilities established in Defence Metallurgical Research Laboratory for mechanical property measurements of MEMS materials were also highlighted.

#### ACKNOWLEDGEMENTS

The author would like to thank Director, Defence Metallurgical Research Laboratory, Hyderabad for permission to publish this paper and to Defence Research & Development Organisation for providing funding for this study.

#### REFERENCES

- Gabriel, K.J. Microelectromechanical systems. *Proceedings IEEE*, 1998, **86**, 1534-535.
- Paula, G. MEMS sensors branch out. *Mechanical Engineering*, 1996, **118**, 64-6.
- Zhou, Q.; Tan, W.; Kim, E.S. & Loeb, G.E. Single and triaxis piezoelectric-bimorph accelerometers. *J. Microelectromech. Syst.*, 2008, **17**, 45-57.
- Nafari, A.; Karlan, D.; Rusu, C.; Svensson, K.; Olin, H. & Enoksson, P. MEMS sensor for *in-situ* TEM atomic force microscopy. *J. Microelectromech. Sys.*, 2008, **17**, 328-33.
- Du, C.-L.; Kao, P.H.; Tai, Y.W. & Wu, C.C. Micro FET pressure sensor manufactured using CMOS-MEMS technique. *Microelectronics Journal*, 2008, **39**, 744-49.
- Hautefeuille, M.; O'Mahony, C.; O'Flynn, B.; Khalfi, K. & Peters, F. MEMS based wireless multisensor for environmental monitoring. *Microelectronics Reliability*, 2008, **48**, 906-10.
- Gilgunn, P.J.; Liu, J.; Sarkar, N. & Fedder, G.K. CMOS-MEMS lateral electrothermal actuator. *J. Microelectromech. Sys.*, 2008, **17**, 103-14.
- Subrahmanyam, G.; Mohanty, A. & Chatterjee, A. Cantilever beam electrostatic MEMS actuators. *J. Micromech. Microeng.*, 2006, **16**, 1800-10.
- Lin, B.C.; King, T.-J. & Muller, R.S. Poly-SiGe MEMS actuators for adaptive optics. *In Proceedings SPIE*, 2006, **6113**, pp. 222-28.
- Shay, B.; Hubbard, T. & Kujath, M. Linear friction microconveyors. *Sensors and Actuators A: Physical*, 2008, **148**, 290-98.
- Epstein, A.H. & Senturia, S.D. Microengineering: Macropower from micromachinery. *Science*, **276**, 1997, 1211-215.
- Zhu, L.J.; Lin, K.L.; Morgan, R.D.; Swaminathan, V.V.; Kim, H.S.; Gurau, B.; Kim, D.; Bal.B.; Masel, R.I. & Shannon, M.A. Integrated micropower source based on a microsilicon fuel cell and microelectromechanical system hydrogen generator. *J. Power Sources*, 2008, **185** 1305-310.
- Duggirala, R.; Polcawich, R.G.; Dubey, M. & Lal, A. Radioisotope thin film fuelled microfabricated reciprocation electromechanical power generator. *J. Microelectromech. Sys.*, 2008, **17**, 837-49.
- Srinivasan, R.; Firebaugh, S.L.; Hsing, I.M.; Riley, J.; Harold, M.P.; Jensen K.F. & Schmidt, M.A. Chemical performance and high temperature characterisation of micromachined chemical reactors. *In International Conference on Solid State Sensors and Actuators*, Chicago, June 1997. pp 163-66.
- Hwang, S.-M; Kwon, O.-J; Ahn, S.-H. & Kim, J.-J. Silicon based microreactor for preferential CO oxidation. *Chem. Eng. J.*, 2009, **146**, 105-11.
- Mei, F.; Parida, P.R.; Jiang, J.; Meng, F.J. & Ekkal, S.V. Fabrication, assembly and testing of Cu and Al based microchannel heat exchangers. *J. Microelectromech. Sys.*, 2008, **17**, 869-81.
- Bisson, C.; Campbell, J.; Cheadle, R.; Chomiak, M.; Lee, J.; Miller, C.; Milley, C.; Pialis, P.; Shaw, S.; Weiss, W. & Widrig, C. A microanalytical device for the assessment of coagulation parameters in whole blood. *In Proceedings Solid State Sensor and Actuator Workshop*, Hilton Head Island, June 1998, pp. 1-6.
- Henry, S.; McAllister, D.V.; Allen, M.G. & Prausnitz, M.R. Microfabricated microneedles: A novel approach to transdermal drug delivery. *J. Pharmaceut. Sci.*, 1998, **87**, 922-25.
- Wang, J. & Wise, K.D. A Hybrid electrode array with built in position sensor for an implantable MEMS based cochlear prosthesis. *J. Microelectromech. Sys.*, 2008, **17**, 1187-198.
- Nisar, A.; Afzulpurkar, N.; Mahaisarariya, B.; & Tuantranont, A. MEMS based micropumps in drug delivery and biomedical applications. *Sensors and Actuators B: Chemical*, 2008, **130**, 917-42.
- Tang, W.C. & Lee, A.P. Defence applications of MEMS. *MRS Bulletin*, 2001, **26**, 318-19.
- Sharpe Jr., W.N.; Yuan, B.; Vaidyanathan R. & Edwards, R.L. New test structures and techniques for measurement of MEMS materials. *In Proceedings SPIE*, **2880**, 1996. pp. 78-91
- Obermeier, E. Mechanical and thermophysical properties of thin film materials for MEMS: Techniques and devices. *In Microelectromechanical structures for materials research. Materials Research Society Symposium*, Boston, 1996, **444**, 39-57.
- Yi, T. & Kim, C.J. Measurement of mechanical properties for MEMS materials. *Meas. Sci. Tech.*, 1999, **10**, 706-16.
- Schweitz, J.A. & Ericson, F. Evaluation of mechanical materials properties by means of surface micromachined structures. *Sensors and Actuators A.: Physical*, 1999, **74**, 126-33.
- Sharpe Jr., W.N. Mechanical properties of MEMS materials: *In MEMS Handbook*. CRC Press, 2001, pp. 3-33.
- Sharpe Jr., W.N. Mechanical properties of MEMS materials. *In MEMS Introduction and Fundamentals*. CRC Press, 2006, pp. 3-1.
- Liu, R.; Wang, H.; Li, X.; Ding, G. & Yang, C. A microtensile method for measuring mechanical properties of MEMS materials. *J. Micromech. Microeng.*, 2008, **18**, 065002.

29. Arzt, E. Size effects in materials due to microstructural and dimensional constraint: A comparative review. *Acta Materialia*, 1998, **46**, 5611-626.
30. Bhushan, B. & Li, X., Nanomechanical characterisation of solid surfaces and thin films. *Int. Mater. Rev.*, 2003, **48**, 125-64.
31. Oliver, W.C. & Pharr, G.M., An improved technique for determining hardness and elastic modulus using load and displacement sensing indentation experiments. *J. Mater. Res.*, **7**, 1992, 1564-583.
32. Han, S.W.; Lee, H.W.; Lee, H.J.; Kim, J.Y.; Kim, J.H.; Oh, C.S.; & Choa, S.H. Mechanical properties of Au films for applications in MEMS/NEMS using microtensile test. *Curr. Appl. Phys.*, 2006, **6**, e81-e85.
33. Sharpe Jr., W.N. & Hemker, K.J., Mechanical testing of free standing thin films. In Materials Research Society Symposium Proceedings, 2002, **687**, pp.292-304.
34. Modlinski, R.; Puers, R. & De Wolf, I., AlCuMgMn microtensile specimens: Mechanical characterisation of materials at micro-scale. *Sensors and Actuators A: Physical*, 2008, **143**, 120-28.
35. Read, D. T. & Dally, J. W. New method for measuring the strength and ductility of thin films. *J. Mater. Res.*, 1993, **8**, 1542-549.
36. Brown, S. B.; Edwards, R. L.; Panth, R.; Bergstrom, J.; Coles, G. & Sharpe Jr., W. N., Mechanical property of silicon nitride thin film. In MRS Symposium B, Boston, 2001. pp. B 9.2-6 .
37. Tsuchiya, T.; Tabata, O.; Sakata, J. & Taga, Y., Specimen size effect on tensile strength of surface micromachined polycrystalline silicon thin films. In Proceedings IEEE 10<sup>th</sup> Annual International Workshop on MEMS, 1997. pp. 529-34.
38. LaVan, D. A.; Tsuchiya, T.; Coles, G.; Knauss, W. G.; Chasiotis, I. & Read, D. Cross comparison of direct tensile testing techniques on SUMMIT polysilicon Films. *ASTM STP 1413*, 2001, 62-71.
39. Sharpe Jr., W.N.; Eby, M.A. & Coles, G. Effect of temperature on the mechanical properties of polysilicon. In Proceedings Transducers, 2001, pp. 1366-369.
40. Sharpe Jr., W. N.; Turner, K.T. & Edwards, R.L. Tensile testing of polysilicon. *Exp. Mechanics*, 1999, **39**, 162-70.
41. Cornella, G.; Vinci, R.P.; Iyer, R.S.; Dauskardt, R.H. & Bravman, J.C. Observations of low cycle fatigue of Al thin films for MEMS applications. In Material Research Society Symposium Proceedings, 1998, **518**, pp. 81-86.
42. Sharpe Jr., W.N.; Yuan, B. & Edwards, R.L. A new technique for measuring the mechanical properties of thin films. *J. Microelectromech. Sys.*, 1997, **6**, 193-99.
43. Sharpe Jr., W. N. An Interferometric strain/displacement measurement system. NASA Technical Memorandum No. NASA TM 101638, 1989.
44. Bucheit, T.; Glass, S.; VaVan, D.; Mani, S.; Friedmann, T. & Sullivan, J. An interferometric strain displacement gage for measuring strain in thin film. *ASME IMECE*, 2001, MAT-8.
45. Chasiotis, I. & Knauss, W.G. Instrumentation requirements in mechanical testing of thin films. In Proceedings Society for Experimental Mechanics, 2000. pp. 56-61.
46. Espinosa, H. D.; Prorok, B. C. & Fischer, M. A novel experimental technique for testing thin films and MEMS. In Proceedings of the SEM Annual Conference on Experimental and Applied Mechanics. Portland, Oregon, 2001.
47. Hong, S.; Weihs, T. P.; Bravman, J. C. & Nix, W.D. Residual stresses in thin films using microcantilever beams In Thin Films: Stresses and Mechanical Properties, edited by J. C. Bravman; W. D. Nix; D. M. Barnett, & D.A. Smith, *Mater. Res. Soc. Proc.*, 1989, **130**, 93-98.
48. Weihs, T. P.; Hong, S.; Bravman, J.C. & Nix, W.D. Mechanical deflection of microcantilevers to measure mechanical properties of thin films. *J. Mater. Res.*, 1988, **3**(5), 931-42.
49. Baker, S.P. & Nix, W.D. Mechanical properties of compositionally modulated Au-Ni thin films using indentation and microbeams. *J. Mater. Res.*, 1994, **9** (12), 3131-144.
50. Florado, J.N. & Nix, W.D. A microbeam method for studying stress-strain relations for metal thin films on silicon substrates. *J. Mech. Phys. Solids*, 2005, **53**, 619-38.
51. Schwaiger, R. Fatigue behaviour of sub-micron Ag and Cu films. University of Stuttgart, 2001. (Ph.D. Dissertation)
52. Paviot, V.M.; Vlassak, J.J. & W.D. Nix, Bulge test for determining mechanical properties of thin films. *Mater. Res. Symp. Proc.*, 1995, **356**, 579-85.
53. Vlassak, J.J. New experimental techniques and analysis methods for the study of the mechanical properties of materials in small volumes. Stanford University, 1994. (PhD Thesis)
54. Vlassak, J.J. & Nix, W.D. A new bulge test technique for the determination of Young's modulus and Poisson's ratio of thin films. *Int. J. Mater. Res.*, 1992, **7**, 3242-252,
55. Doerner, M.F.; Gardner, D.S. & Nix, W.D. Plastic properties of thin films on substrates as measured by sub-micron indentation hardness and substrate curvature measurements. *J. Mater. Res.*, 1986, **1**, 845-51.
56. Sinha, A.K. & Sheng, T.T. The temperature dependence of stresses in aluminium films on oxidized silicon substrates. *Thin Solid Films*, 1978, **48**, 117-26.
57. Muhlstein, C.L., Brown, S.B. & Ritchie, R.O., High cycle fatigue of polysilicon thin film in laboratory air. In Material Research Society Symposium Proceedings. 2001, **657**, pp. EE 5.8.1-EE5.8.6.

58. Baxter, L.K. *In* Capacitive sensors: design and applications. IEEE, New York, 1997.
59. Freeman, D.M.; Aranyosi, A.J.; Gordon, M.J. & Hong, S.S. Computer micro-vision system for MEMS. *In* Solid-State Sensor and Actuator Workshop Technical, 1998. pp. 150-55.
60. Bouzakis, K.D.; Asimakopoulos, A. & Batsiolas, M. *Surf. Coat. Technol.*, 2008, **202**, 5929-935.
61. Zhang, G.P.; Sun, K.H.; Zhang, B.; Gong, J.; Sun, C. & Wang, Z. G. Tensile and fatigue strength of ultrathin Cu films. *Mater. Sci. Eng. A*, 2008, **483-484**, 387-90.
62. Bae, J.S; Oh, C.S.; Park, K.S.; Kim, S.K. & Lee, H.J. Development of high cycle fatigue test system and its application to thin aluminium film. *Eng. Fract. Mech.*, 2008, **75**, 4958-964.

#### Contributor



**Dr Samir V. Kamat** completed his BTech in Metallurgical Engineering from Indian Institute of Technology (IIT), Kharagpur in 1985 and his PhD in Materials Science and Engineering from Ohio State University, Columbus, Ohio, USA in 1988. He is working at the Defence Metallurgical Research Laboratory, Hyderabad, since 1989. His areas of interest are: mechanical behaviour of materials in MEMS, mixed-mode fracture and microstructure-mechanical properties correlations in advanced metallic alloys.